



## Current subsidence rates due to compaction of Holocene sediments in southern Louisiana

T. A. Meckel,<sup>1</sup> U. S. ten Brink,<sup>1</sup> and S. Jeffress Williams<sup>1</sup>

Received 14 March 2006; revised 26 April 2006; accepted 2 May 2006; published 14 June 2006.

[1] Relative contributions of geologic and anthropogenic processes to subsidence of southern Louisiana are vigorously debated. Of these, shallow sediment compaction is often considered dominant, although this has never been directly observed or effectively demonstrated. Quantitative understanding of subsidence is important for predicting relative sea level rise, storm surge flooding due to hurricanes, and for successful wetland restoration. Despite many shallow borings, few appropriate stratigraphic and geotechnical data are available for site-specific calculations. We overcome this by determining present compaction rates from Monte Carlo simulations of the incremental sedimentation and compaction of stratigraphies typical of the Holocene of southern Louisiana. This approach generates distributions of present compaction rates that are not expected to exceed 5 mm/yr, but may locally. Locations with present subsidence rates greater than the predicted maximum probable shallow compaction rates are likely influenced by additional processes. **Citation:** Meckel, T. A., U. S. ten Brink, and S. J. Williams (2006), Current subsidence rates due to compaction of Holocene sediments in southern Louisiana, *Geophys. Res. Lett.*, 33, L11403, doi:10.1029/2006GL026300.

### 1. Introduction

[2] The conversion of wetlands to open water occurs at alarming rates in coastal Louisiana, where subsidence contributes significantly to relative sea level rise of  $\sim 1$  cm/yr [Penland and Ramsey, 1990]. The value of wetlands for providing habitat and buffering storm surge has encouraged efforts to identify and mitigate subsidence (and other) processes that cause wetland loss. With the variety of geologic (compaction, faulting, isostasy) and anthropogenic (subsurface fluid withdrawal, forced surface drainage, dredging) processes involved [Penland *et al.*, 1990, Day *et al.*, 2000; Morton *et al.*, 2005], the current pattern of wetland loss [Williams *et al.*, 2003] is challenging to explain. Active contributions from any single process have previously not been well constrained, and their spatial and temporal variability is even more difficult to determine. Given the stratigraphic complexities and diverse processes contributing to subsidence, it is difficult to extrapolate subsidence rate estimates or observations over significant distances. Yet planning and implementing cost-effective coastal and wetland restoration in Louisiana requires accurate estimates on scales of 100's of  $m^2$  to 1000's of  $km^2$ .

[3] Previous research suggests that current subsidence rates increase with thicker Holocene sediments [Penland and Ramsey, 1990; Roberts *et al.*, 1994]. However, we lack quantitative analyses of the compaction history of these sediments, and therefore cannot accurately predict such contributions to present subsidence rates. Constraints on shallow compaction rates are clearly needed.

[4] Previous attempts to estimate compaction at time and thickness scales similar to the Holocene of Louisiana [Pizzuto and Schwendt, 1997; Kooi *et al.*, 1998; Kooi, 2000] have either been site-specific or employed extremely generalized stratigraphy. Despite the large number of borings within the Holocene of Louisiana, geologic and geotechnical data sufficient for detailed modeling are still unavailable for much of the delta plain.

[5] To overcome this limitation, we use stochastic Monte Carlo simulations to capture the anticipated range of present compaction rates for a wide range of present stratigraphic thicknesses, stratigraphic compositions, and accumulation times. For stratigraphies with similar present compacted thicknesses and accumulation times, a distribution of modeled present compaction rates is generated. We provide a graphic tool for determining the maximum probable present compaction rates for any location where the Holocene thickness and time of accumulation are known. We then compare expected compaction rates to observed subsidence rates.

### 2. Data

#### 2.1. Stratigraphy

[6] Shallow stratigraphy in the lower Mississippi River delta is comprised of latest Pleistocene-age substratum overlain by Holocene-age topstratum [Fisk, 1954]. The coarser, more homogenous substratum is relatively incompressible (resists penetrometers [Kuecher *et al.*, 1993]), and the compaction of the heterogeneous stratigraphy of the topstratum is of primary interest. Holocene (topstratum) thickness varies across the delta plain (Figure 1), thickening in the paleovalley of the Mississippi River.

[7] Detailed stratigraphic information is unavailable for much of the delta plain and stratigraphic heterogeneity leads to uncertainty where borings are unavailable. The most readily available data from a regional perspective is the Holocene stratigraphic thickness. The duration of accumulation (age of the base of the topstratum) is not known everywhere, but is considered  $< 12$  k.y. regionally. Thus, we model present compaction rates varying these two parameters and treat stratigraphic heterogeneity stochastically.

#### 2.2. Geotechnical Parameters

[8] Geotechnical parameters used to describe the physical properties of consolidating sediments are compressibility

<sup>1</sup>U.S. Geological Survey, Woods Hole, Massachusetts, USA.

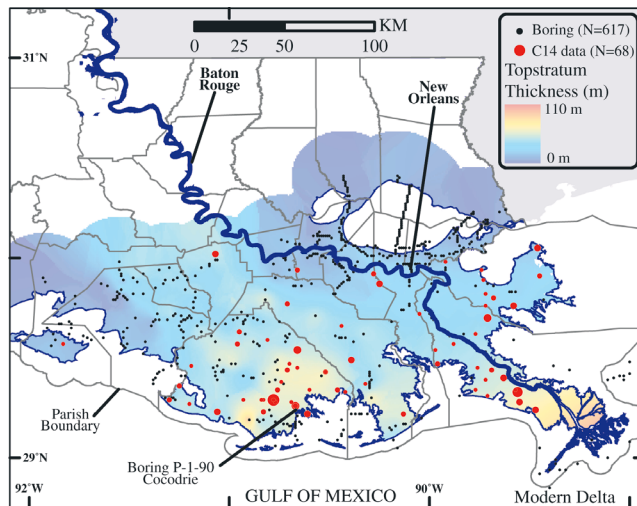


**Figure 1.** Holocene sediment thickness in southern Louisiana (parishes outlined). Black dots are 617 borings [May *et al.*, 1984; Kulp *et al.*, 2002] used to interpolate thickness by spherical kriging. Red dots are 68  $^{14}\text{C}$  sample locations with radius scaled to radiometric subsidence rate minus modeled maximum probable Holocene compaction rate ( $P_{90}$ ).

(b), initial porosity ( $\Phi_0$ ), grain density ( $\rho$ ), and the constants  $c_1$  and  $c_2$  relating permeability to porosity (see below). Laboratory oedometer tests typically constrain  $b$ ,  $\Phi_0$ , and  $\rho$ . Porosity-permeability relationships are established empirically [Bryant *et al.*, 1975]. Kuecher [1994] provides geotechnical data and sample locations for five facies typically comprising the modern delta plain: peat, bar sand, natural levee, bay mud, and pro-delta mud (Table 1; initial values). Geotechnical parameters change with progressive burial and are updated throughout the calculations.

### 3. Numerical Methods

[9] We employ the compaction calculations of Kooi and de Vries [1998], which solve one-dimensional, multi-lithology compaction models using a finite difference technique. The application of these calculations to subsidence problems in The Netherlands has been demonstrated by Kooi *et al.* [1998] and Kooi [2000]. Kooi and de Vries [1998] use the fundamental concepts of Darcy flow law, Terzaghi's [1943] principle of effective stress ( $\sigma_{\text{eff}} = \sigma - p_n$ ), and a constitutive relationship between porosity and effective stress [ $\Phi = \Phi_0 \exp(-b \cdot \sigma_{\text{eff}})$ ]. The relationship of permeability ( $k$ ) with  $\Phi$  is modeled as  $k = k_r \cdot 10^{(-c_1 + \Phi c_2)}$ , where  $k_r$  is a reference permeability ( $1 \text{ m}^2$  here). For other constants (e.g., fluid density and compressibility) we follow Kooi and de Vries [1998]. The rate of vertical displacement of the uppermost stratigraphic surface due to compaction of the thickening depositional column was determined incrementally throughout deposition, but we focus here on the present rate.

#### 3.1. Monte Carlo Simulations

[10] Monte Carlo methods [Jensen *et al.*, 1997] provide a statistically powerful way to evaluate the likelihood of a

particular result. Given our limited detailed knowledge of stratigraphy throughout coastal Louisiana, these methods allow a broad range of facies order, sedimentation rates, and accumulation times to be considered. It is our premise that by modeling an exhaustive range of possible stratigraphies, any observed stratigraphy will have a present compaction rate somewhere on our model distributions.

[11] Synthetic stratigraphies are generated by randomly selecting layer properties from predefined distributions with observed (or otherwise conservative) ranges. Cyclic deposition of a suite of facies is commonly cited in delta systems [Roberts, 1997]. However, we note that other 'cyclic' systems such as cyclothems and carbonate platforms do not have stacking patterns that are statistically distinguishable from stochastic models [Wilkinson *et al.*, 2003]. Without data from Louisiana demonstrating otherwise, we model stratigraphy without imposing cyclicality.

[12] Layer properties that are assigned randomly are thickness, sedimentation rate, and geotechnical parameters (facies). The thickness of each layer is selected from an exponential distribution [Wilkinson *et al.*, 2003]. The average bed thickness of the distribution used for all stratigraphic models is defined to be that which is observed in a 64 m boring (P-1-90, Figure 1 [Roberts *et al.*, 1994]). There are 13 unique units, providing an average bed thickness of  $\sim 4.9$  m. However, we have determined that compaction rates are not sensitive to variability in average bed thickness. The sedimentation rate probability density function  $f(x)$  is modeled with a two-parameter gamma distribution

$$f(x) = \frac{1}{\beta^\alpha \Gamma(\alpha)} x^{\alpha-1} \cdot e^{-x/\beta}$$

such that the distribution average ( $\alpha \cdot \beta$ ) is equal to the average sedimentation rate for the uncompacted thickness and time parameters of each stratigraphic model. Gamma distributions avoid the undesired outcome of frequently assigning extremely low sedimentation rates that result from an exponential distribution. Nondeposition is effectively modeled when extremely low sedimentation rates are selected. We do not explicitly decrease average sedimentation rates toward the present [Giosan and Bhattacharya, 2005], but do permit such models to be generated and evaluated.

[13] Initial geotechnical properties for each layer were determined by randomly selecting one of the five model facies. The number of layers and facies in each stratigraphy is unrestricted. Models are considered to incorporate the actual stratigraphic heterogeneity in the delta plain, although statistics of observed deposits are unavailable for comparison.

**Table 1.** Initial Geotechnical Parameters for Uncompacted Facies [Kuecher, 1994]

Facies	$C_1$	$C_2$	$\Phi_0$	$b, \text{Pa}^{-1}$	$\rho, \text{kg/m}^3$
Peat	20.0	8.0	0.88	1.0E-06	1.12E+03
Sand bar	14.0	4.0	0.57	1.0E-07	1.88E+03
Natural levee	20.0	6.0	0.42	5.0E-07	1.78E+03
Bay mud	22.0	8.0	0.61	4.0E-06	1.40E+03
Pro-delta mud	22.0	7.0	0.78	1.0E-06	1.22E+03

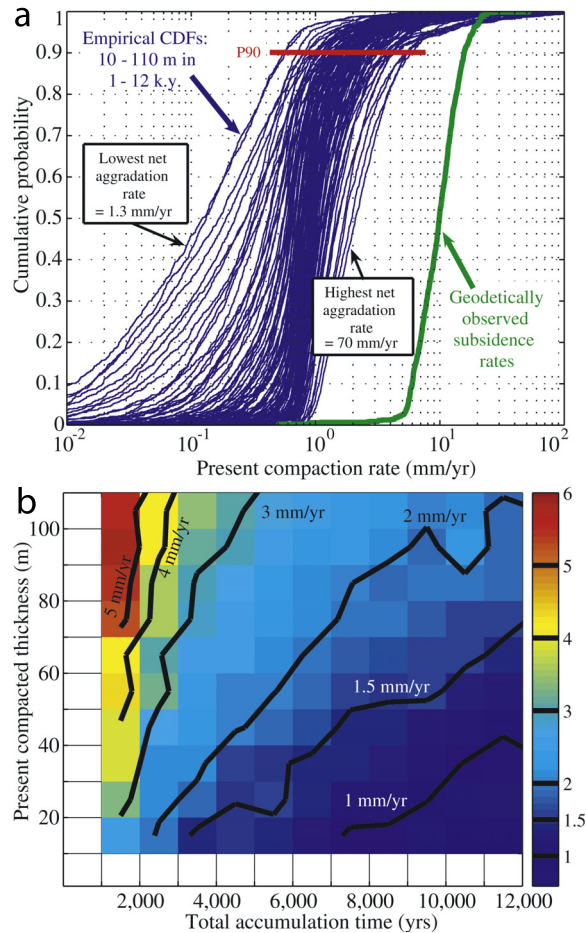


**Figure 2.** (a) Cumulative distribution functions (CDF) for modeled stratigraphies. Red line spans  $P_{90}$  compaction rates plotted in Figure 2b in their associated bin. Green curve is CDF of 875 geotechnically determined subsidence rates [Shinkle and Dokka, 2004]. (b)  $P_{90}$  compaction rates vary systematically with present compacted thickness and accumulation time. Black lines contour constant  $P_{90}$  compaction rates.

[14] The parameter space of thickness (10–200 m) and accumulation time (1–12 k.y.) was divided into 209 bins ( $19 \times 11$ ), each spanning 10 m and 1 k.y. Uncompacted stratigraphies up to 200 m had to be modeled in order to consider all stratigraphies that could compact to a present thickness in our range of interest (<110 m; Figure 1). Each bin was populated with 1,000 stochastically-generated uncompacted stratigraphies, which were then made to incrementally accumulate and compact to arrive at a compacted thickness and present compaction rate.

#### 4. Results

[15] A cumulative probability distribution function (CDF) of the modeled present compaction rates was generated for stratigraphies in each bin between 10–110 m of compacted thickness with accumulation time between 1–12 k.y. (110 blue curves in Figure 2a, each having >1000 stratigraphies). The cumulative probability (y-axis) is the fraction of the models in a bin with present

compaction rates less than the corresponding rate on the x-axis. The 90<sup>th</sup> percentile ( $P_{90}$ ) rates of each CDF are arbitrarily considered to be the maximum probable (not actual) present compaction rate, and are plotted with their corresponding compacted thickness and accumulation times in Figure 2b. The reader can use Figure 2b to estimate  $P_{90}$  for any Holocene stratigraphy in southern Louisiana (Figure 1) using only the present thickness and time of accumulation.

#### 5. Discussion

[16] Stochastic models indicate that compaction rates need not relate directly to thickness. A range of rates is possible for a given thickness, and ranges of compaction rates for different thicknesses overlap (Figure 2a). However,  $P_{90}$  rates do increase with thickness (Figure 2b), and CDFs shift to higher ranges with increased net aggradation rate (Figure 2a), as expected.

[17] Modeled present compaction rates are generally low (Figure 2). Locally, compaction rates may be significant. Present compaction rates can exceed 5 mm/yr where >70 m accumulated in <2 k.y. (Figure 2b). A distributary mouth bar at South West Pass prograded 17 km in 200 years producing a sand body >80 m thick [Coleman, 1988]. Although we did not model this exact stratigraphy,  $P_{90}$  compaction rates there are likely to be >5 mm/yr (left of red area in Figure 2b). Yet, these conditions are atypical of the entire coastal plain.

[18] Observed subsidence rates > $P_{90}$  (for a given thickness and time) may relate to: geotechnical properties beyond the scope of our models, stochastically (but perhaps not geologically) rare stratigraphic accumulations, or the influence of other processes in addition to shallow compaction. Locations where subsidence cannot be

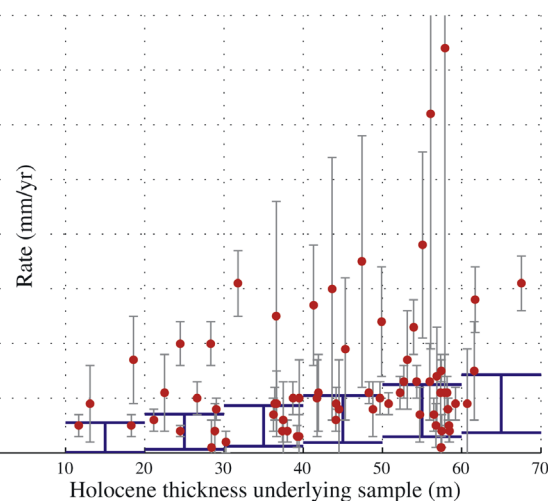


**Figure 3.** Comparison of subsidence rates determined from 68  $^{14}\text{C}$  samples (red dots; Figure 1.) with the expected  $P_{10}$ – $P_{90}$  range of compaction rates (blue lines) for the thickness of Holocene underlying the  $^{14}\text{C}$  samples. Differences between  $^{14}\text{C}$  rates and modeled compaction distributions indicate processes in addition to Holocene compaction are likely to contribute to subsidence for at least half of the sites.



explained by shallow compaction should be investigated for contributions of deeper compaction, faulting, or fluid withdrawal.

[19] We compare our modeled compaction rates with subsidence rates derived from radiometrically-dated ( $^{14}\text{C}$ ) peat samples [Kulp, 2000] (all samples corrected for age in calendar years before present and Holocene sea level rise). We chose a subset of samples with ages <1 k.y. and burial depths <3 m (N = 68; Figure 1) which minimize potential correction errors and presumably reflect only recent subsidence. The Holocene thickness beneath the sample depth is derived from Figure 1 minus the recorded sample depth. Using the sub-sample thickness and Figure 2, the radiometric subsidence rate can be compared with expected model compaction rates. If we assume that the age of the base of the topstratum is everywhere 12 k.y., then the comparison indicates that 49% of the radiometric subsidence rates are greater than corresponding  $P_{90}$  compaction rates, and only 18% are below  $P_{50}$  (Figure 3). If subsidence at these locations was due only to compaction of the underlying Holocene-age sediments, we would expect  $\sim 10\%$  of radiometric subsidence rates  $>P_{90}$  and  $\sim 50\%$   $<P_{50}$ . Even if the assumption of the age of the base of topstratum is relaxed to include any age between 2–12 k.y., 27% of radiometric subsidence rates are still  $>P_{90}$  and 27% are  $<P_{50}$ . The fact that many more radiometric subsidence rates are higher than the expected distribution of modeled compaction rates suggests that processes other than shallow compaction likely contribute to subsidence in at least half of the sites. Figure 1 shows no apparent geographic pattern to locations where radiometric subsidence rates are  $>P_{90}$  compaction rates.

[20] Another set of subsidence rates in the same region was derived from 875 geodetic observations [Shinkle and Dokka, 2004]. The range of geodetic rates (rightmost CDF in Figure 2a) is an order of magnitude larger than both our estimated compaction rates and the observed radiometric subsidence rates. Shinkle and Dokka [2004] discuss potential caveats of the geodetic data. Assuming the geodetic data correctly measure recent subsidence rates, processes in addition to Holocene compaction contribute overwhelmingly (up to 90%) to geodetic rates. Differences in the length of observation periods (decades vs. 100s of years) may explain some differences between the range of geodetic and radiometric subsidence rates.

[21] The delta plain is unlikely to be composed of only five facies with internally constant initial geotechnical parameters. Better data on the distribution of geotechnical parameters are needed. Our results are maximum values because we assume sedimentation occurred until the present. If significant sedimentation ceased with artificial levee construction on the Mississippi River (<200 yrs ago), then actual maximum compaction rates would be lower. While most compaction occurs in the shallow subsurface, deeper compaction also contributes to (increases) present subsidence rates, but has not yet been quantified.

## 6. Summary

[22] Contemporary compaction of Holocene sediments (topstratum) is unlikely to contribute more than a few mm/

yr to present subsidence rates, but may be more significant locally. For a specific location, observed subsidence rates greater than the 90th percentile of the appropriate modeled compaction rate distribution likely include processes in addition to shallow compaction. Our methodology is readily applicable to other deltas with similar subsidence and flooding problems.

[23] **Acknowledgments.** We thank H. Kooi for providing compaction routines, and A. Solow, B. Wilkinson, L. Lake, and J. Jensen for geo-statistical discussions. D. Twichell and D. Lavoi (USGS), and T. Törnqvist (Tulane Univ.) provided helpful reviews.

## References

- Bryant, W. R., W. Hottman, and P. Trabant (1975), Permeability of unconsolidated and consolidated marine sediments, Gulf of Mexico, *Mar. Geotechnol.*, 1(1), 1–14.
- Coleman, J. M. (1988), Dynamic changes and processes in the Mississippi River delta, *Geol. Soc. Am. Bull.*, 100(7), 999–1015.
- Day, J. W., Jr., L. D. Britsch, S. R. Hawes, G. P. Shaffer, D. J. Reed, and D. Cahoon (2000), Pattern and process of land loss in the Mississippi Delta: A spatial and temporal analysis of wetland habitat change, *Estuaries*, 23(4), 425–438.
- Fisk, H. N. (1954), Sedimentary framework of the modern Mississippi Delta, *J. Sediment. Petrol.*, 24(2), 76–99.
- Giosan, L., and J. Bhattacharya (Eds.) (2005), *River Deltas: Concepts, Models and Examples*, Spec. Publ. SEPM Soc. Sediment. Geol., 83, 508 pp.
- Jensen, J. L., L. W. Lake, P. W. M. Corbett, and D. J. Goggin (1997), *Statistics for Petroleum Engineers and Geoscientists*, 390 pp., Prentice Hall, Upper Saddle River, N. J.
- Kooi, H. (2000), Land subsidence due to compaction in the coastal area of the Netherlands: Role of lateral fluid flow and constraints from well-log data, *Global Planet. Change*, 27, 207–222.
- Kooi, H., and J. J. de Vries (1998), Land subsidence and hydrodynamic compaction of sedimentary basins, *Hydrol. Earth Syst. Sci.*, 2(2–3), 159–171.
- Kooi, H., P. Johnston, K. Lambeck, C. Smither, and R. Molendijk (1998), Geological causes of recent ( $\sim 100$  yr) vertical land movement in the Netherlands, *Tectonophysics*, 299, 297–316.
- Kuecher, G. L. (1994), Geologic framework and consolidation settlement potential of the Lafourche Delta, topstratum valley fill; Implications for wetland loss in Terrebonne and Lafourche Parishes, Louisiana, Ph.D. thesis, 346 pp., La. State Univ., Baton Rouge.
- Kuecher, G. L., N. Chandra, H. H. Roberts, J. H. Suhayda, S. J. Williams, S. P. Penland, and W. J. Autin (1993), Consolidation settlement potential in south Louisiana, in *Coastal Zone '93: Proceedings of the Eighth Symposium on Coastal and Ocean Management*, pp. 175–192, Am. Soc. of Civ. Eng., New York.
- Kulp, M. A. (2000), Holocene stratigraphy, history, and subsidence: Mississippi River delta region, north-central Gulf of Mexico, Ph.D. thesis, 336 pp., Univ. of Ky., Lexington.
- Kulp, M. A., P. Howell, S. Adiau, S. Penland, J. Kindinger, and S. J. Williams (2002), Latest Quaternary stratigraphic framework of the Mississippi River Delta region, *Trans. Gulf Coast Assoc. Geol. Soc.*, 52, 573–582.
- May, J. R., L. D. Britsch, J. B. Dunbar, J. P. Rodriquez, and L. B. Wloinski (1984), Geologic investigation of the Mississippi River deltaic plain: Vicksburg Mississippi, *Tech. Rep. GL-84-15*, 67 plates, U.S. Army Eng. Waterw. Exp. Stn., Vicksburg, Miss.
- Morton, R. A., J. C. Bernier, J. A. Barras, and N. F. Ferina (2005), Rapid subsidence and historical wetland loss in the Mississippi delta plain: Likely causes and future implications, *U.S. Geol. Surv. Open File Rep.*, 2005-1216, 116 pp.
- Penland, S., and K. E. Ramsey (1990), Relative sea-level rise in Louisiana and the Gulf of Mexico: 1908–1988, *J. Coastal Res.*, 6(2), 323–342.
- Penland, S., H. H. Roberts, S. J. Williams, A. H. Sallenger, D. R. Cahoon, D. W. Davis, and C. G. Groat (1990), Coastal land loss in Louisiana, *Trans. Gulf Coast Assoc. Geol. Soc.*, 40, 685–699.
- Pizzuto, J. E., and A. E. Schwendt (1997), Mathematical modeling of autocompaction of a Holocene transgressive valley-fill deposit, Wolfe Glade, Delaware, *Geology*, 25(1), 57–60.
- Roberts, H. H. (1997), Dynamic changes of the Holocene Mississippi River Delta plain: The delta cycle, *J. Coastal Res.*, 13(3), 605–627.
- Roberts, H. H., A. Bailey, and G. J. Kuecher (1994), Subsidence in the Mississippi River delta—Important influences of valley filling by cyclic

- deposition, primary consolidation phenomena, and early diagenesis, *Trans. Gulf Coast Assoc. Geol. Soc.*, 44, 619–629.
- Shinkle, K. D., and R. K. Dokka (2004), Rates of vertical displacement at benchmarks in the lower Mississippi valley and the northern Gulf Coast, *NOAA Tech. Rep. NOS/NGS 50*, 147 pp.
- Terzaghi, K. (1943), *Theoretical Soil Mechanics*, 510 pp., John Wiley, Hoboken, N. J.
- Wilkinson, B. H., G. K. Merrill, and S. J. Kivett (2003), Stratal order in Pennsylvanian cyclothems, *Geol. Soc. Am. Bull.*, 115(9), 1069–1087.
- Williams, S. J., J. M. Reid, V. A. Cross, and C. F. Polloni (2003), Coastal erosion and wetland change in Louisiana, *USGS Digital Data Ser. DDS-79*, U.S. Geol. Surv., Woods Hole, Mass.
- 
- T. A. Meckel, U. S. ten Brink, and S. J. Williams, U.S. Geological Survey, Woods Hole, MA 02543, USA. (tmeckel@usgs.gov)